Dev Genes Evol (2011) 221:209–223
DOI 10.1007/s00427-011-0373-5

ORIGINAL ARTICLE

BMP signals and the transcriptional repressor *BLIMP1* during germline segregation in the mammalian embryo

Clas Hopf · Christoph Viebahn · Bernd Püschel

Received: 4 April 2011 / Accepted: 28 July 2011 / Published online: 1 September 2011

Abstract Molecular factors and tissue compartments involved in the foundation of the mammalian germline have been mainly described in the mouse so far. To find mechanisms applicable to mammals in general, we analyzed temporal and spatial expression patterns of the transcriptional repressor *BLIMP1* (also known as *PRDM1*) and the signaling molecules *BMP2* and *BMP4* in perigastrulation and early neurulation embryos of the rabbit using whole-mount in situ hybridization and high-resolution light microscopy. Both *BMP2* and *BMP4* are expressed in annular domains at the boundary of the embryonic disc, which—in contrast to the situation in the mouse—partly belong to intraembryonic tissues. While *BMP2* expression begins at (pregastrulation) stage 1 in the hypoblast, *BMP4* expression commences—distinctly delayed compared to the mouse—diffusely at (pregastrulation) stage 2; from stage 3 onwards, *BMP4* is expressed peripherally in hypoblast and epiblast and in the mesoderm at the posterior pole of the embryonic disc. *BLIMP1* expression begins throughout the hypoblast at stage 1 and emerges in single primordial germ cell (PGC) precursors in the posterior epiblast at stage 2 and then in single mesoderm cells at positions identical to those identified by PGC-specific antibodies. These expression patterns suggest that function and chronology of factors involved in germline segregation are similar in mouse and rabbit, but higher temporal and spatial resolution offered by the rabbit demonstrates a variable role of bone morphogenetic proteins and makes "blimping" a candidate case for lateral inhibition without the need for an allantoic germ cell niche.

Keywords Primordial germ cell niche · Gastrulation · PRDM1 · Rabbit

Communicated by A. Kispert

C. Hopf · C. Viebahn · B. Püschel (✉)
Department of Anatomy and Embryology, Center of Anatomy,
Georg-August-University Göttingen,
Kreuzbergring 36,
37075 Göttingen, Germany
e-mail: bpuesch@gwdg.de

Introduction

Mechanisms of germline segregation during early embryonic development are known at the cellular and molecular levels in intricate detail deduced from elegant and comprehensive studies in the mouse (for review, see Saitou and Yamaji 2010). Looking across the mammalian phylum, however, the "earliest common denominator" in the development of the germline still appears to be evidence of single primordial germ cells (PGCs) loosely arranged in the stalk of the yolk sac in mouse, rabbit, and human embryos during early neurulation stages (mouse: Chiquoine 1954; rabbit: Schäfer-Haas and Viebahn 2000; human: Witschi 1948; reviews: McLaren 2003; Chuva de Sousa Lopes and Roelen 2008). In mouse, early PGCs are defined as individual cells with a strong expression of tissue non-specific alkaline phosphatase (Chiquoine 1954), and transplantation experiments identified a PGC founder population of approximately 45 cells in the allantoic mesoderm of the 7.2-day-old mouse embryo (Lawson and Hage 1994). Mouse and rabbit embryos provided evidence for the segregation of PGC precursors from the primitive streak epiblast close to the extraembryonic ectoderm or trophoblast (Lawson and Hage 1994; Tam and Zhou 1996; Anderson et al. 2000; Weckelmann et al. 2008) from where they subsequently migrate to posterior extraembryonic regions, such as the base of the developing allantois (mouse: Snow 1981; Anderson et al. 2000) and the

proximal yolk sac endoderm (mouse: Anderson et al. 2000; rabbit: Schäfer-Haas and Viebahn 2000). Molecular genetic studies in the mouse now point to extracellular signals of the bone morphogenetic protein (BMP) family and to the transcriptional repressors *Blimp1* (*Prdm1*) and *Prdm14* which drive segregation of germ cells from somatic cell lines and repression of the somatic gene program (Saitou and Yamaji 2010). Known as the main players of mammalian germline determination to date, these factors form the molecular proof of the inductive (epigenetic) principle of germline segregation in mammals (Ohinata et al. 2009) and thus for a program fundamentally different from germline development by preformation on the basis of maternal determining factors in other animal phyla (review: Extavour and Akam 2003).

Intriguingly, extraembryonic tissue plays a double role in the epigenetic mode of PGC formation because signals responsible for initiating germline segregation appear to reside in early extraembryonic tissues and, as has long been known (cf. Nieuwkoop and Sutasurya 1979; Anderson et al. 2000), PGCs are transferred transiently to extraembryonic tissues such as the base of the allantois and the yolk sac (see above). Molecular factors known to be involved in this role of the extraembryonic tissues belong to the group of BMPs in the transforming growth factor-beta family of intercellular signaling molecules. In the mouse, the *Bmp4* signal can be detected between 5.5 and 6.5 days post coitum (dpc) in the proximal region of the extraembryonic ectoderm (trophoblast) close to the epiblast; up to 7.5 dpc *Bmp4* is also expressed in the mesoderm of amnion, yolk sac, and allantois (Lawson et al. 1999; Ying et al. 2000). In PGCs themselves, *Bmp4* has been detected by single-cell gene expression analysis (Saitou et al. 2002; Kurimoto et al. 2008) but not by histochemical LacZ staining of $Bmp4^{LacZneo}$ embryos (Lawson et al. 1999). However, knock-out experiments show that the *Bmp4* signal is essential for PGC development: homozygotic mutants do not develop any PGCs and, in heterozygotic mutants, PGC numbers are reduced by about 62% (Lawson et al. 1999). *Bmp2* mRNA, on the other hand, originates in the visceral endoderm (hypoblast) and its RNA can first be detected between 6.0 and 6.5 dpc with the strongest expression residing in the region of the forming primitive streak at the border between extraembryonic ectoderm and epiblast (Coucouvanis and Martin 1999; Ying and Zhao 2001). In knock-out experiments with *Bmp2*-loss-of-function mutants, the number of PGCs is highly reduced (but not abolished) both in homozygotic and heterozygotic mutants (Ying and Zhao 2001). Coincident loss of one allele for *Bmp2* and *Bmp4* shows an additive effect on the reduction of the PGCs (Ying and Zhao 2001). The *Bmp8b* signal, finally, originates in the extraembryonic ectoderm only (RNA detected from 5.5 dpc onwards; Ying et al. 2000) and is thought to control visceral endoderm (hypoblast) differentiation, thereby modulating inhibition of *Bmp4* by the anterior visceral endoderm (AVE; Ohinata et al. 2009). *Bmp8b* has a direct influence on PGC development, as their number is reduced in homo- and heterozygote *Bmp8b*-loss-of-function mutants (Ying et al. 2000). Experiments with combined *Bmp4*/*Bmp8b* mutants show a non-additive effect of these two molecules (Ying et al. 2000). That BMPs are, indeed, the relevant extraembryonic factors producing the regulative effects of transplantation experiments on PGC development (Yoshimizu et al. 2001) was finally proven by Chuva de Sousa Lopes et al. (2007). Taken together, BMP signals initiate the phosphorylation of intracellular signal molecules (Smad1, Smad5, and Smad4) which seems to create a situation in which PGC precursors can be segregated from somatic cell lineages (Chang and Matzuk 2001) and, as one of the first signs of germ cell competence, pluripotent proximal epiblast cells start to express *fragilis* (*Ifitm3*; Saitou et al. 2002), although only a small number of these cells will then proceed to become definite PGCs (Tanaka and Matsui 2002).

The transcriptional repressor *Blimp1* was first described for its function in the differentiation of antibody producing plasma cells (Turner et al. 1994), but in the context of germline differentiation it is probably the earliest marker for a definite PGC fate (Ohinata et al. 2005): Approximately six cells of a *fragilis* expressing cluster in the mouse egg-cylinder start to express *Blimp1* at 6.25 dpc, and by 6.5 dpc, the number of *Blimp1* expressing proximal epiblast cells increases to 16, all of which are now considered to be definite PGC precursors. Homozygote *Blimp1*-loss-of-function mutants develop PGC-like cells which lie in a cluster but do not show typical signs of proliferation or migration and have an increased rate of apoptosis (Ohinata et al. 2005; Vincent et al. 2005). In heterozygote mutants, only the number of PGCs is reduced (by about 78%), whereas the proliferation rate and subsequent migration are not affected. With regard to germline-specific gene regulation, the early *Blimp1* expressing proximal epiblast cells show a repression of *Hox1b* and other mesodermal (and somatic) master regulators, like *Fgf8* and *Snail* (Ancelin et al. 2006), before pluripotency-associated genes such as *Sox2* (Yabuta et al. 2006) and *Nanog* (Yamaguchi et al. 2005) are upregulated. Consequently, the PGC-like cells of the *Blimp1* mutants have an inconsistent repression of *Hox1a* and *Hox1b* and fail to express PGC markers such as *stella*, *sox2*, and *nanog*. Putative PGCs in normal embryos may show a transient coexpression of somatic and germ cell markers, which underlines the important role of *Blimp1* for the repression of the somatic cell fate and PGC development (Kurimoto et al. 2008; Chuva de Sousa Lopes and Roelen 2008).

Early extraembryonic tissues known to be the sources for PGC-inducing factors vary markedly between mammalian species; for some of them—the rodent *Bmp4* expressing extraembryonic ectoderm being just one example—an

equivalent structure is difficult to find in non-rodent mammals including the human embryo (cf. Kaufman 1992; O'Rahilly and Müller 1987). In addition, developmental timing and topography of the allantois, the transient residence of PGCs in the mouse, is highly divergent amongst mammals (Mossman 1937). For example, early allantoic mesoderm is almost non-existent in many non-rodents with delayed implantation while—possibly due to the rodent-specific egg-cylinder morphology—the murine allantois grows to a comparatively large size "prematurely" and its root comes to lie unusually close to the anterior pole of the embryo. Mechanisms for suppressing the influence of anterior signals on PGC development (e.g., *Bmp8b* suppression of AVE differentiation: Ying et al. 2001) may have evolved specifically in rodents only. To attain a general model for mammalian PGC development, mammal model organisms need to be investigated which manage without a notable allantois anlage during gastrulation, the likely developmental phase of germline segregation (see Saitou and Yamaji 2010). The rabbit may be considered a suitable species in this respect, as it is to date the only mammal with delayed allantois formation in which PGCs can be confidently traced back to their source in the primitive streak (Schäfer-Haas and Viebahn 2000; Weckelmann et al. 2008). Using the germline-specific epitope PG2, a triangular domain containing about 20 single cells can be identified in the mesoderm close to the posterior half of the mature primitive streak (at stage 4); subsequently, this domain is separated into two symmetrical flanks near the embryonic disc border containing between 60 and 100 PGCs on either side of the primitive streak. This topography and dynamics of PGC formation in the rabbit will be used here as references for an analysis of signals specifying germline differentiation in mammals. Furthermore, analyzing BMP expression in a non-rodent may help to define extraembryonic domains (or their equivalent structures) and their dynamic development during the early gastrulation stages and germline development.

Materials and methods

Animals and tissues

Embryos were obtained from naturally mated 3-month-old New Zealand White rabbits (Lammers, Euskirchen), which had been stimulated by an intramuscular injection of 2× 180 IU Predalon® (Organon, Oberschleissheim, Germany) and 100 IU Intergonan® (Intervet, Unterschleißheim, Germany) as described previously (Weckelmann et al. 2008). Pregnant animals were killed by an intravenous injection of a lethal dose (90 mg per kilogram of body weight) of Narcoren® (Merial, Halbergmoss, Germany). Preimplantation blastocysts (6.0 to 6.5 dies post coitum—dpc) were flushed out of the dissected uterine horns using warm (37°C) phosphate-buffered saline (PBS), while older embryonic stages (beyond 6.5 dpc) where dissected from separated implantation chambers using fine scissors (Idkowiak et al. 2004; Schäfer-Haas and Viebahn 2000). After washing in PBS and removal of a surrounding zona pellucida, isolated embryos were either frozen in liquid nitrogen for later RNA extraction or fixed for 1 h in 4% paraformaldedhyde (PFA in PBS). Subsequently, the fixed embryos were either dehydrated and stored in ethanol at −20°C until their utilization in whole-mount in situ hybridization or used for whole-mount immunofluorescence. Embryonic staging of the rabbit embryos was performed using a dark field microscope according to morphological criteria described by Viebahn et al. (2002) and Blum et al. (2007).

Generation of the rabbit cDNA probes

A 658-bp cDNA probe of rabbit *BMP4* was kindly provided by Christina Karcher (Forschungszentrum Karlsruhe, Eggenstein-Leopoldshafen, Germany). The sequence was found to be identical to the published database entries for rabbit *BMP4* (corresponding to nucleotides 408 to 1181 of the published sequence; GenBank XM_002718254.1 and Ensembl ENSOCUT00000011093; calculated length of the probe is 774 bp) except for a small fragment of 116 bp (corresponding to nucleotides 573–688), which was missing in the probe. Because reasons for this difference were not examined further, we can only speculate that it might result from a—so far unknown—alternative spliced mRNA (the missing bases locate in the predicted exon 2 of the database entry Ensembl ENSOCUT00000011093) or from cloning of a defective cDNA. However, the perfect match of two parts of the probe with database sequences consisting of 165 and 493 neighboring bases respectively, made for a suitable probe for whole-mount in situ hybridization.

Rabbit cDNA probes of *BMP2* and *BLIMP1* were isolated from embryonic RNA using reverse transcriptase PCR. Briefly, total RNA was extracted from five 6.2 dpc rabbit embryos according to the manufacturer's protocol using the RNeasy Mini Kit (Qiagen, Hilden, Germany). Up to 5 μg embryonic total RNA was oligo dT primed and reverse transcribed in a single reaction using 200 U of a Moloney murine leukemia virus reverse transcriptase at 42°C as recommended by the supplier (RevertAid™ H Minus Reverse Transcriptase, Fermentas, St. Leon-Roth, Germany).

Either the published sequence (rabbit *BMP2*, GenBank NM_001082650.1) or aligned cDNA sequences of human, mouse, rat, chimpanzee, rhesus monkey, dog, and cow were utilized to select at least two pairs of "nested" primers—

specific (*BMP2*) or degenerated (*BLIMP1*)—which were used in different combinations. One microliter of the reverse transcription was applied in a standard 50-µl PCR reaction (75 mM Tris–HCl (pH 8.8 at 25°C), 20 mM $(NH_4)_2SO_4$, 0.01% (*v*/*v*) Tween 20, 2 mM $MgCl_2$, 0.2 mM dNTPs, 0.2 to 1 µM primers, 1.25 U recombinant Taq polymerase; Fermentas, St. Leon-Roth, Germany) performing 35 cycles at 95°C for 30 s, 55°C or 60°C for 30 s, 68°C for 3 min. PCR products of the correct size were cloned in pGEM®-T Easy (Promega, Mannheim, Germany) and sequenced on both strands. Successful primer combinations were as follows: *BMP2* (875 bp; nucleotides 219–1,093 of GenBank NM_001082650.1): 5′-CGAGTTCGAGTTGCGGTTGC-3′ (forward) and 5′-CATGGTTAGTGGAGTTCAGG-3′ (reverse). *BLIMP1* fragment A (721 bp; corresponding to nucleotides 390–1,110 of Ensembl ENSOCUT00000015492): 5′-CGGCACCTCCGTGCARGCNGARGC-3′ (forward) and 5′-CAGGGAGGCCTTCAGGAARTCYTCNGG-3′ (reverse). *BLIMP1* fragment B (435 bp; corresponding nucleotides 1,803–2,237 of Ensembl ENSOCUT00000015492): 5′ CCTGATCAAGAACAAGCGGAAYATGACNGG-3′ (forward) and 5′-TGGCACTGGGCGCAYTTRTGNGG-3′ (reverse). High values of homology (99.7% with rabbit *BMP2*, GenBank NM_001082650.1; 98.8% with a predicted rabbit *BLIMP1* cDNA sequence derived from genomic sequences—Ensembl ENSOCUT00000015492—and between 83% and 91% with *BLIMP1* homologues of other species) with published database sequences confirmed the identity of the cloned cDNA probes.

In situ hybridization and histology

cRNA probes for in situ hybridization were generated by PCR from intact plasmid DNA containing the relevant cDNAs using the DIG-RNA labeling mix as specified by the manufacturer (Roche, Mannheim, Germany). In situ hybridization was performed at 70°C as described previously by Weisheit et al. (2002) and Idkowiak et al. (2004). The hybridized cRNA probe was visualized using alkaline phosphatase coupled to an antibody directed against digoxigenin and the BM purple solution (both Roche, Mannheim, Germany). The color reaction was allowed to proceed at room temperature in the dark for up to 7 days until no further accumulation of the blue precipitate was detectable. The stained embryos were spread in Mowiol 4-88 (Hoechst, Frankfurt, Germany) beneath a cover glass and photographed with a stereomicroscope before they were embedded in Technovit 8100® (Heraeus-Kulzer, Wehrheim, Germany) as described previously (Idkowiak et al. 2004). For detailed examination of the histology and the localization of the gene expression, serial sections of 5 µm in thickness prepared with a glass knife in sagittal or transverse planes of at least three embryos per gene and stage were analyzed at high magnification using Normarski contrast (DIC).

Successful in situ hybridization of a specific cRNA probe produces blue staining of the cytoplasm surrounding an unstained or at most weakly stained center representing the position of the cell nucleus. Intensively stained cells are often observed next to unstained tissues demonstrating a good signal to noise ratio of the method. Different staining intensities, characterized either as strong or weak expression in the description, represent a rough estimate of the amount of mRNA present in a particular cell or tissue.

Whole-mount immunofluorescence

Whole-mount immunofluorescence was carried out in a microtiter plate as described in detail elsewhere (Püschel and Viebahn 2010; Weckelmann et al. 2008). Briefly, paraformaldehyde-fixed rabbit embryos were transferred using a glass Pasteur pipette in a minimal liquid volume (approximately 10 µl) between wells containing 100 µl incubation solution each. All incubations were performed—unless otherwise indicated—at room temperature. Unspecific binding sites were saturated by two subsequent incubation steps (15 min each) using PBS containing 0.1% (*v*/*v*) Triton X-100 (Roche, Germany) and 1% (*v*/*v*) normal goat serum (Sigma, Germany). The following antibody solutions and washing buffers differ by the content of normal goat serum only, which was 0.1% (*v*/*v*) instead. To detect the primordial germ cells in the rabbit embryos, a 1:100 dilution of the primary monoclonal anti-PG2 antibody (Viebahn et al. 1998) was administered for 3 h (or for 16 h at 4°C) followed by three consecutive washing steps (5 min each). Subsequently, a Cy3-conjugated goat anti-mouse IgG (2.5 µg/ml; Dianova, Hamburg, Germany) was employed as secondary antibody for 3 h followed by three washing steps. Cell nuclei were counterstained with 4′,6-diamino-2-phenylindole (DAPI, 1 µg/ml in PBS; Serva, Heidelberg, Germany) for 2 min, and the embryonic discs were washed and mounted in Mowiol 4-88 on regular microscope slides. High-resolution photomicrographs were taken at different fluorescent channels with a Leica TCS SP2 confocal laser scanning microscope using a 63× Plan-APO objective (NA 1.3). To examine the localization of stained cells, image stacks of the posterior pole of the embryonic disc were recorded. The blue (DAPI) and the red channel (PG2) were merged and processed using ImageJ software (version 1.43; Abramoff et al. 2004) to extract and visualize an orthogonal (*x*-*z*) section of a region of interest relative to the plane of recorded images of the stack.

Results

BMP2 expression

While in stage 0 rabbit blastocysts no *BMP2* expression is detected (not shown), approximately 50% of stage 1 embryos show *BMP2*-expressing cells in a ring-like domain at the border between the embryonic disc and the extraembryonic tissue (Fig. 1A). As in previous and subsequent stages, the embryonic disc border is morphologically defined through a difference in cellular height between the cylindrical or cuboidal epiblast cells and the squamous trophoblast cells (cf. Fig. 1F). Details of the ring-like domain mirror the emerging anterior–posterior axial differentiation characteristic for this stage: Near the anterior pole of the embryonic disc, *BMP2*-positive cells lie more densely packed than near the posterior margin; extraembryonically they are surrounded by another, somewhat wider ring-like domain of more dispersed *BMP2*-positive cells, inside the disc only few cells are *BMP2*-positive. At stage 2 (Fig. 1B), which is characterized by a markedly increased disc size, the ring-like domain is slightly broader when compared to stage 1 (Fig. 1A); in many specimens, the domain still shows an anterior–posterior gradient in the density of the positive cells. Sagittal sections of stage 1 (Fig. 1F) and stage 2 (not shown) reveal that the BM purple staining is confined to the cytoplasm of hypoblast and yolk sack cells only (Fig. 1H, I), whereas epiblast and trophoblast cells (Fig. 1H, I) show no staining. The ring-like area in the dorsal view (Fig. 1A, B) is mainly formed by three to five neighboring hypoblast cells localized at or near the border between epiblast and trophoblast cells. These hypoblast cells have a distinct cuboidal appearance compared to the almost flat configuration of the neighboring yolk sac epithelial cells. At the anterior margin, which is characterized by a dense packing of hypoblast cells—representing the anterior marginal crescent (AMC, Fig. 1F, H; cf. Fig. 1I)—two to three *BMP2*-expressing hypoblast cells locate outside the border of the epiblast and extend beneath the neighboring trophoblast (Fig. 1H); at the posterior margin, on the other hand, strong *BMP2*-expressing hypoblast cells are found predominantly within the margins of the embryonic disc only (Fig. 1I). Anteriorly, *BMP2*-expressing hypoblast cells lie close to predominantly unstained, more densely packed cuboidal hypoblast cells which, however, are part of the anterior marginal crescent (Fig. 1F). Besides *BMP2* expression at the margins of the embryo, there are also single or small groups of *BMP2*-positive cells which are loosely disseminated in the hypoblast and yolk sac epithelium (arrowheads in Fig. 1F).

At the onset of gastrulation (as seen by the emergence of mesoderm cells and the density of the primitive streak at stage 3, Fig. 1C), the ring-like *BMP2* expression domain appears broader at the posterior end of the embryonic disc compared to the width of the staining at the anterior and lateral margins. Sagittal sections of the posterior extremity (Fig. 1J) show that the staining is mainly due to an expression in the hypoblast cells, while most of the emerging mesoderm cells (Fig. 1J) do not show clear *BMP2* expression. Anterior hypoblast cells show similar intensive staining and cuboidal compact morphology as at stage 2 (not shown). At stage 4 (Fig. 1D), the number of *BMP2*-expressing cells has much increased compared to the earlier stages: The extraembryonic domain immediately surrounding the embryonic disc shows a dense *BMP2* expression and sagittal sections (Fig. 1G, L, M) reveal that there are two sorts of *BMP2*-expressing yolk sac epithelial cells (Fig. 1M): close to the embryonic disc border cells are mainly cuboidal (bracket in Fig. 1M) and at a greater distance to the embryonic disc *BMP2* positive cells have a more flat morphology. Furthermore, some intra- and extraembryonical mesoderm cells near the border at the posterior end of the embryo show a weak to moderate *BMP2* expression as well (Fig. 1L). Similar to the stages 1 to 3, overlaying epiblast and trophoblast cells do not show *BMP2* expression (Fig. 1L, M), but a second noticeable *BMP2* expression domain consists of intensively stained and partially aggregated cells inside the embryonic disc surrounding the node in a cloud-shaped structure (Fig. 1D) of mesoderm cells (Fig. 1K) next to unstained hypoblast and overlaying epiblast cells.

At stage 5 (Fig. 1E), nearly all the extraembryonic tissue expresses *BMP2* while the intraembryonic staining is confined to a crescent-like area in the anterior part of the embryonic disc. Similar to the expression at stage 4, sagittal sections show *BMP2* staining in cuboidal (Fig. 1N, O) and flat yolk sac epithelial cells (not shown). Close to the anterior (Fig. 1N) and lateral (not shown) margin of the embryo cells of the ventral layer and of the overlaying mesoderm express *BMP2*, while cells of the dorsal layer and the trophoblast are not stained. The intraembryonic crescent-like *BMP2* expression is localized mainly in the mesoderm layer and in the prechordal plate anterior to the notochord (Fig. 1E, N). At the posterior margin of the embryo (Fig. 1O), a weak *BMP2* expression is found in cuboidal cells of the ventral layer resembling the appearance of the adjacent *BMP2*-positive yolk sac epithelial cells. In addition, a weak *BMP2* expression is also present in the extraembryonic mesoderm, while the intraembryonic mesoderm is not stained.

BMP4 expression

Comparison of different pregastrulation stages of the rabbit blastocysts analyzed here reveals the first weak *BMP4* expression to occur at the stage 2 while the earlier stages 0

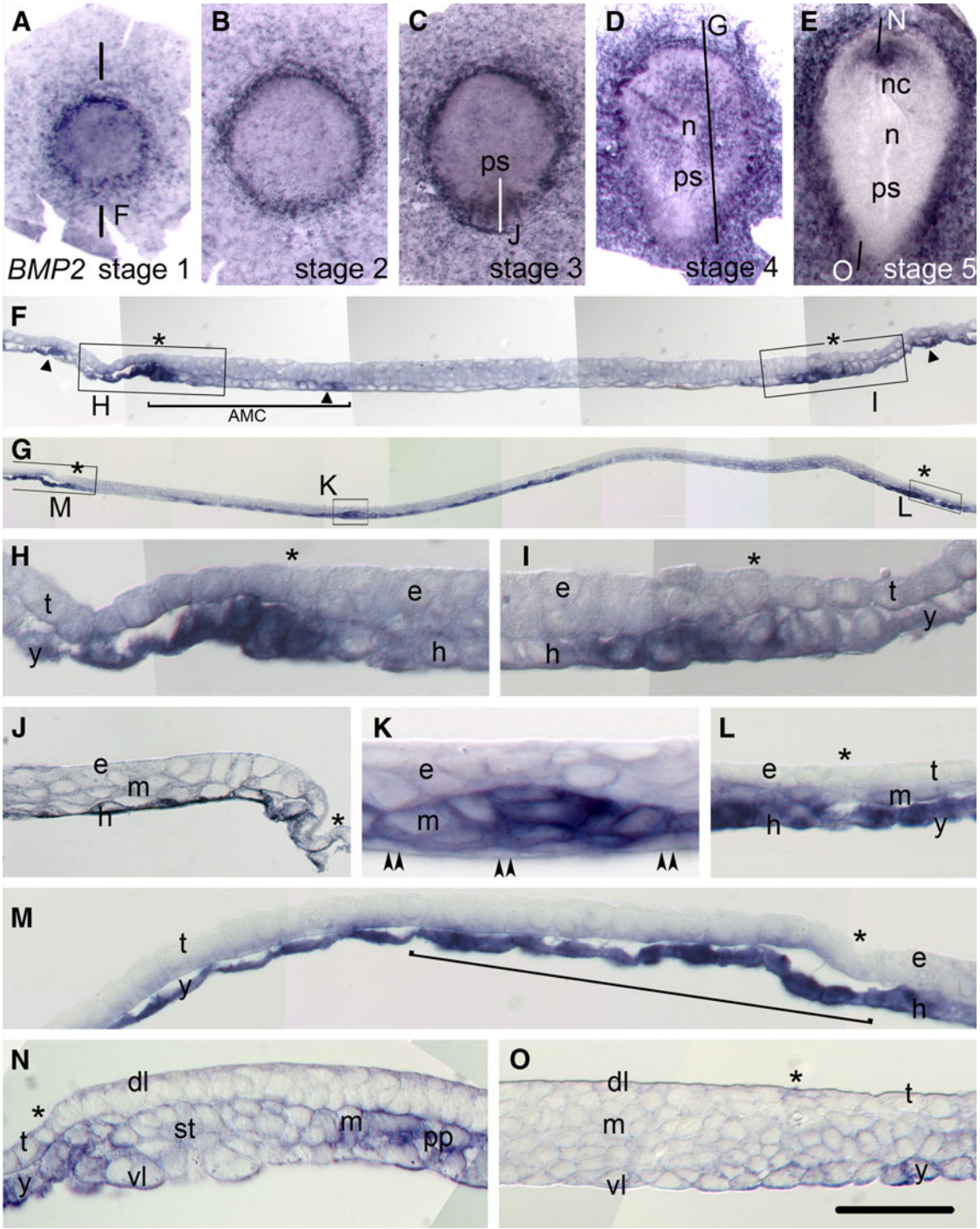

Fig. 1 Expression of *BMP2* in rabbit embryonic discs: en face views (**A**–**E**) oriented with the anterior pole to the top and 5-μm Technovit® sections at low (**F**, **G**) and high magnification (**H**–**O**) from stage 1 to stage 5 (recovered at 6.0–7.2 dpc, respectively) as analyzed by in situ hybridization. All sections are oriented with the anterior pole to the left and the epiblast (*e*) to the top. *Bars* and *letters* refer to positions of sections shown and in **C**–**E** their length represents the length of the transverse section shown in **J**, **G**, **N**, and **O**. Boxes in **F** and **G** indicate magnified details in **H**, **I**, and **K**–**M**; *asterisks* mark the border of the embryonic disc. Cell layers and structures are marked as follows: *e* = epiblast, *h* = hypoblast, *t* = trophoblast, *y* = yolk sac epithelium, *m* = mesoderm, *dl* = dorsal layer, *vl* = ventral layer, *n* = Hensen's node, *ps* = primitive streak, *nc* = notochordal process, *st* = position of the future septum transversum, and *pp* = prechordal plate. *Single arrowheads* in **F** mark loosely disseminated BMP2-expressing cells; *double arrowheads* in **K** indicate weakly stained hypoblast cells beneath strongly labeled mesodermal cells. *Scale bar*: 730 μm (**A**–**F**), 100 μm (**G**), 90 μm (**F**), 40 μm (**J**, **N**, **O**), 33 μm (**L**, **M**), 20 μm (**H**, **I**), and 18 μm (**K**)

and 1 are not stained (not shown). Single *BMP4*-positive cells at stage 2 (Fig. 2A) are dispersed across the area of the embryonic disc and some also aggregated at the border between embryonic and extraembryonic tissues. In sections, these *BMP4*-expressing cells are found in both layers of the embryonic disc, the hypoblast and epiblast (not shown, cf. Fig. 2H). At the onset of gastrulation at stage 3 (Fig. 2B), the *BMP4* expression is most prominently visible in anterior

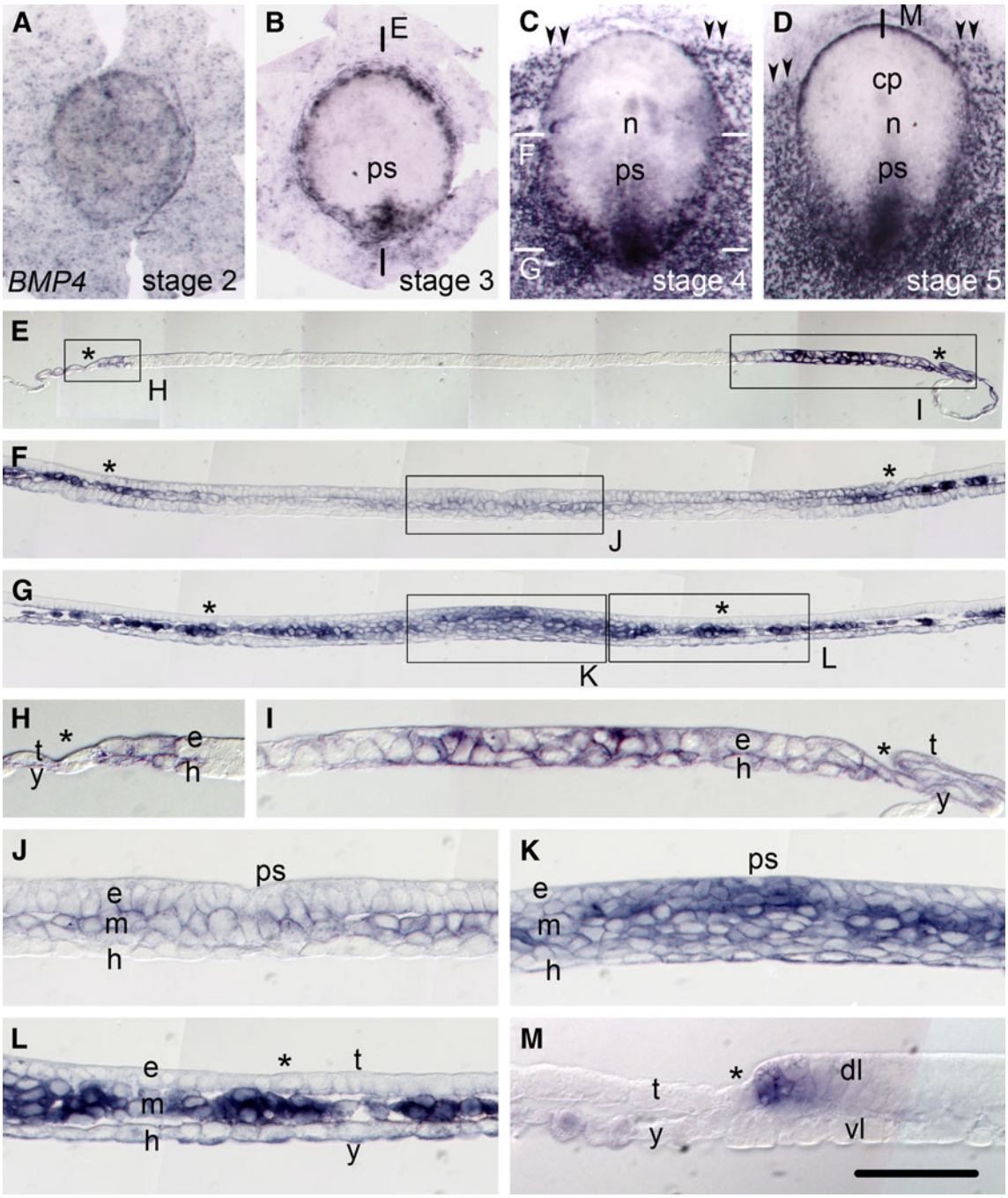

Fig. 2 Localization of *BMP4* in rabbit embryonic discs from stage 2 to stage 5 (at 6.2–7.2 dpc). En face view of in situ hybridized embryos (**A**–**D**) oriented with the anterior pole to the top and 5-μm Technovit® sections at low (**E**–**G**) and high magnification (**H**–**M**). Sagittal sections (**E**, **H**, **I**, **M**) are oriented with the anterior pole to the left and epiblast (*e*) or dorsal layer (*dl*) to the top. Transverse sections (**F**, **G**, **J**–**L**) are aligned with the epiblast to the top. *Bars* and *letters* refer to positions of sections shown and in **D** their length represents that of the transverse section shown in **M**. Boxes in **E**–**G** indicate magnified details shown in **H**-**L**; *asterisks* mark the border of the embryonic disc. *e* = epiblast, *h* = hypoblast, *t* = trophoblast, *y* = yolk sac epithelium, *m* = mesoderm, *dl* = dorsal layer, *vl* = ventral layer, *n* = Hensen's node, *ps* = primitive streak, and *nc* = notochordal process. *Scale bar*: 700 μm (**A**–**D**), 100 μm (**F**, **G**), 60 μm (**E**), 40 μm (**J**–**M**), and 20 μm (**H**, **I**)

and lateral areas in a narrow ring-like domain at the border of the embryonic disc, whereas at the posterior pole this expression appears broader and more crescent-like with the highest intensity occurring at the posterior extremity of the primitive streak. A weak and more dispersed expression can be seen in the extraembryonic tissue surrounding the embryonic disc. Sagittal sections (Fig. 2E) of anterior and lateral areas show that this *BMP4* expression is confined to two or three neighboring cells of the epiblast and the hypoblast; these cells line the embryonic disc border between epiblast and trophoblast or hypoblast and yolk sac epithelium, respectively (Fig. 2H). Sagittal sections of the posterior area of the embryonic disc (Fig. 2E) show that the strong *BMP4* expression at the posterior extremity of the primitive streak (Fig. 2I) lies in all three cell layers, the epiblast, the emerging mesodermal cells, and the hypoblast. In the immediate neighborhood to this strong staining, there is a weaker expression, similar to the intensity at the anterior border (Fig. 2H), and this is found in epiblast and hypoblast cells at the posterior margin of the embryo. At stages 4 and 5, strong *BMP4* expression is found in the posterior half of the primitive streak and along the posterior boundary of the embryonic disc (Fig. 2C, D). Sections of the embryo (Fig. 2G; not shown) display a strong *BMP4* expression in the epiblast and in the neighboring mesoderm of the posterior half of the primitive streak (Fig. 2K), whereas the epiblast cells of the anterior half of the primitive streak do not express *BMP4* and the underlying mesoderm show a weak *BMP4* expression only (Fig. 2F, J). Intraembryonically—and more prominently so extraembryonically—mesodermal cells show diverse intensities of *BMP4* expression with variably sized groups of strong expressing cells intermingled with those displaying an intermediate or weak expression (Fig. 2G, L). This expression pattern produces a salt-and-pepper appearance in the extraembryonic tissue of the en face views of stage 4 and 5 embryonic discs (cf. Figs. 2C, D).

Remarkably, the *BMP4* expression defines several mesodermal subdomains near the anterior and lateral embryonic disc borders from stage 4 onwards: (1) The embryonic mesoderm is *BMP4*-negative, but extraembryonic mesoderm—morphologically indistinguishable from embryonic mesoderm at this stage—shows the strong but patchy mesodermal expression described above. (2) Anteriorly, the extraembryonic *BMP4* expression reaches to a transverse plane immediately posterior to the anterior margin at stage 4, and this coincides with the transverse extremity of anterior mesoderm migration (sections not shown). At stage 5, *BMP4* expression reaches a similar transverse plane, but mesoderm reaches further forward (Fig. 2M) but lacks *BMP4* expression in this most anterior (and extraembryonic) domains. Also at the anterior margin of the embryonic disc, there is a narrow marginal domain (Fig. 2C, D) in the dorsal cell layer of the embryonic disc (presumably surface ectoderm) which consists of approximately three to four adjacent cells expressing *BMP4* with intermediate intensity at stage 4 (not shown) and strong intensity at stage 5 (Fig. 2M).

BLIMP1 expression

At stage 0, only few cells are stained with the *BLIMP1* cRNA probe (Fig. 3A) and sections (Fig. 3E) show that these cells belong to epiblast or hypoblast of the embryonic disc (Fig. 3J) or to yolk sac epithelium or trophoblast cells outside the extraembryonic disc (Fig. 3K), respectively. Detailed comparison of all stage 0 embryonic discs—which by definition do not show morphological signs of anterior–posterior axial differentiation—reveals that the largest embryonic discs (here defined as belonging to "stage 0+") have a preferential localization of stained cells in the one half of the embryonic disc which—compared with the expression pattern at stage 1 (Fig. 3B)—corresponds to the anterior pole of the embryo (not shown). At stage 1, *BLIMP1* is found to be expressed at the center and in a crescent-shaped area near the anterior margin of the embryonic disc (Fig. 3B). Sections of these embryonic discs confirm the morphological axial differentiation (presence of the AMC in the hypoblast) and reveal that *BLIMP1* expression now occurs in the hypoblast only; epiblast and the extraembryonic tissue show no expression (Fig. 3F, L). At stage 2, most of the *BLIMP1*-positive cells localize in a ring-like area near the border between embryonic disc and extraembryonic tissue while only a minority of dispersed *BLIMP1*-positive cells can be found in the center of the embryo (Fig. 3C). Sections show that most of the *BLIMP1* reaction is confined to the hypoblast (Fig. 3G, M), except for the posterior pole of the embryonic disc, where strong *BLIMP1* expression is found in single marginal epiblast cells (Fig. 3H, N).

With the onset of gastrulation at stage 3, there is a salt-and-pepper pattern of strong *BLIMP1* expression in a crescent-shaped domain overlying the emerging primitive streak at the posterior pole of the embryonic disc (Fig. 3D). Sections reveal the *BLIMP1* expressing cells belong to epiblast cells at or near the embryonic disc border (Fig. 3I, O), whereas epiblast cells inside the disc do not show *BLIMP1* expression (cf. Fig. 3O, P). In addition, there are single dispersed *BLIMP1*-expressing cells in the mesoderm (inside and lateral to the primitive streak) and in the hypoblast (Fig. 3O, P). The ring-shaped *BLIMP1* expression domain at the anterior and lateral border of the embryo and the expression domain within the disc display different intensities varying between a stronger staining similar to that seen at stage 2 (Fig. 3C, G) and a weaker intensity as presented in Fig. 3D. However, the *BLIMP1* expression at the border and within the anterior

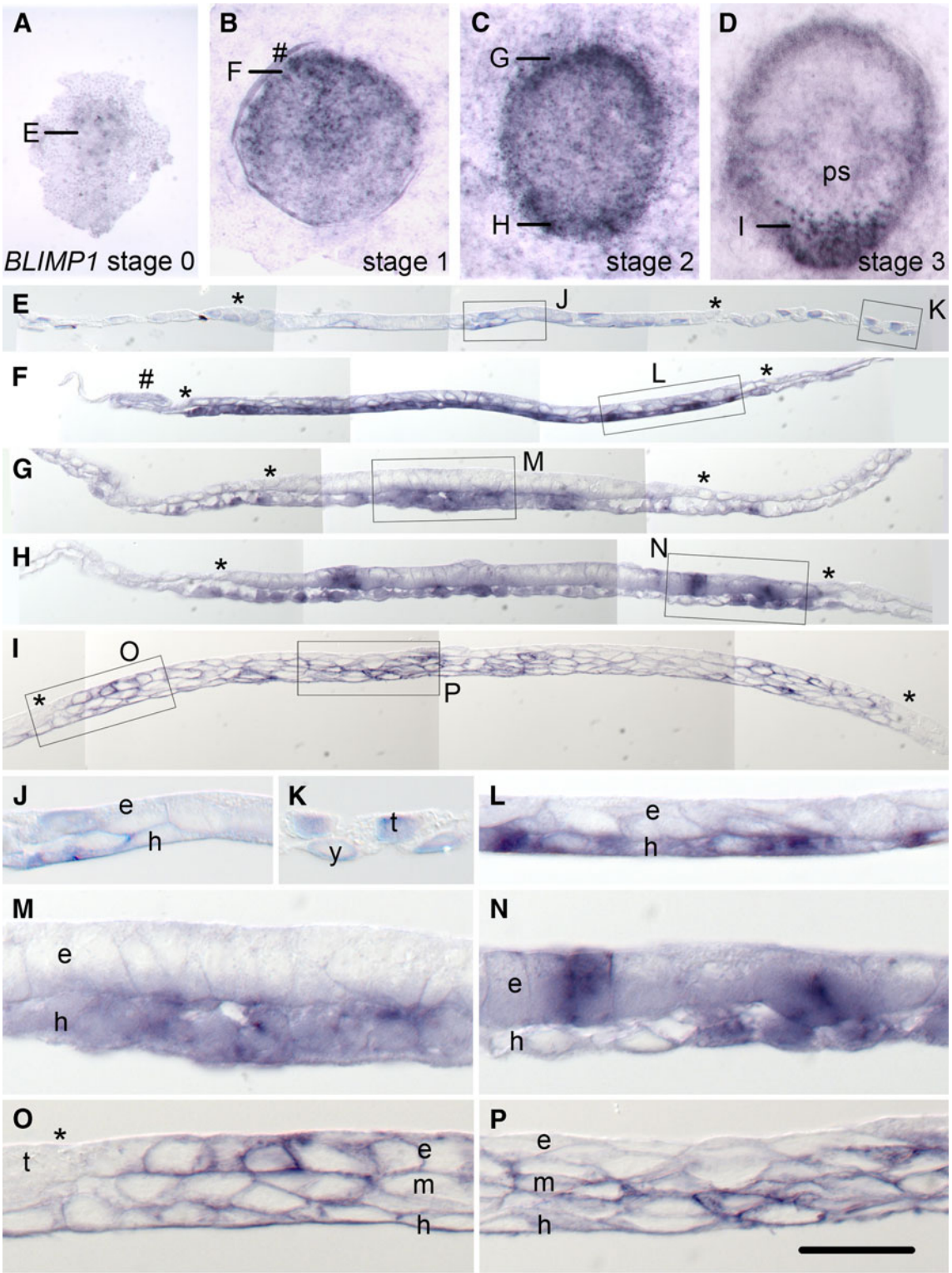

Fig. 3 Distribution of *BLIMP1* in perigastrulation stages of embryonic discs from stages 0–3 (at 6.0–6.5 dpc). En face views of in situ hybridized embryos oriented with the anterior pole to the top (**B**–**D**); at stage 0 (**A**), which lack an unequivocal morphological axis, the presumptive anterior pole is oriented to the top as well. Transverse 5-μm Technovit® sections at low (**E**–**I**) and high magnification (**J**–**P**) are oriented with the epiblast (*e*) to the top. *Bars* and *letters* refer to positions of the sections (**E**–**I**) where boxes indicate magnified details shown in **J**–**P**. *Asterisks* mark the border of the embryonic disc; *number sign* refers to tissue processing artifact. *e* = epiblast, *h* = hypoblast, *t* = trophoblast, *y* = yolk sac epithelium, *m* = mesoderm, and *ps* = primitive streak. *Scale bar*: 500 μm (**A**–**D**), 80 μm (**E**), 70 μm (**F**–**I**), and 20 μm (**J**–**P**)

two thirds of the embryonic disc is still localized to hypoblast cells only (not shown).

At stage 4 (Fig. 4A), similar to the earlier stages described before, there is *BLIMP1* expression in the hypoblast inside the disc and at the border between embryonic and extraembryonic tissue (not shown). Cross sections of the posterior pole reveal strong *BLIMP1* expression in single mesodermal cells which in some cases

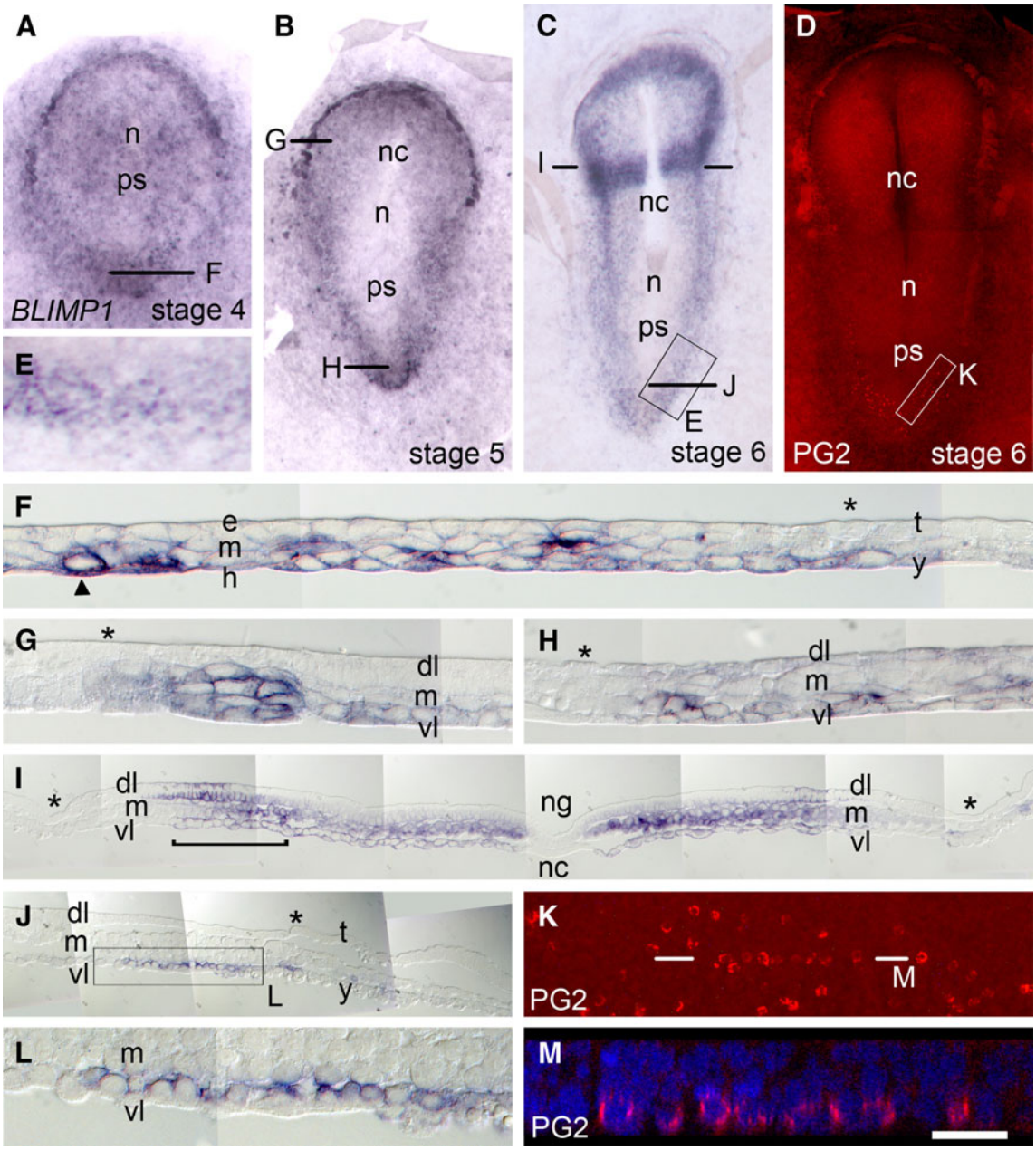

Fig. 4 *BLIMP1* expression in gastrulation and neurulation stages (stages 4 to 6, recovered at 7.0–7.6dpc, respectively) and a comparison with immunolocalized primordial germ cells at stage 6. En face view of in situ hybridized (**A**–**C**) or immunostained (**D**) embryos oriented with the anterior pole to the top. Transverse 5-µm Technovit® sections of in situ hybridized embryos are displayed at low (**I**, **J**) and high magnification (**F**–**H**, **L**) with the epiblast (*e*) or the dorsal layer (*dl*) oriented to the top. *Bars* and *letters* refer to positions of sections shown and those labeled with **F**–**H** and **J** represent the length of the transverse section shown in the corresponding image; the box in **J** indicates a magnified detail shown in **L**. In immunofluorescence images (**D**, **K**, **M**), the cytoplasm of primordial germ cells is stained in red (germ cell-specific antibody PG2) while cell nuclei can be recognized in blue (DAPI). The boxed area in **C** and **D** is visualized at greater detail in **E** and **K**. A computerized projection of a selected *z*-plane, generated from a confocal image stack recorded between the bars in **K**, is shown at greater detail in **M**. *Asterisks* mark the border of the embryonic disc. *e* = epiblast, *h* = hypoblast, *t* = trophoblast, *y* = yolk sac epithelium, *m* = mesoderm, *dl* = dorsal layer, *vl* = ventral layer, *n* = Hensen's node, *ps* = primitive streak, *nc* = notochordal process, and *ng* = neural groove. *Scale bar*: 450 µm (**A**–**C**), 400 µm (**D**), 150 µm (**E**), 80 µm (**I**, **J**), 70 µm (**K**), 30 µm (**M**), and 25 µm (**F**–**H**, **L**)

associate closely with hypoblast cells (arrowhead in Fig. 4F). While there is no *BLIMP1* expression detectable in the epiblast cells (Fig. 4F), the underlying hypoblast cells show a weak expression similar to the one observed at stage 3 (cf. Figs. 3O and 4F). At stage 5, the posterior crescent-shaped domain of *BLIMP1*-positive cells of stage 3 or 4 embryos (Figs. 3D and 4A) is elongated anterior-laterally and is now almost completely separated into two branches (Fig. 4B). Sections through these branch-like domains show single *BLIMP1*-positive mesoderm cells partially associated with weakly stained hypoblast cells (Fig. 4H). As observed at earlier stages, the general border of the embryo is marked by a weak *BLIMP1* expression in the hypoblast (Fig. 4B, G). At the anterior border, however, the embryonic disc of stages 4 and 5 is surrounded by a thin band of distinctly *BLIMP1*-positive mesoderm and hypoblast cells which coincides with the location of blood island precursors (not shown and Fig. 4G, respectively).

At stage 6, additional and prominently strong *BLIMP1* expression appears in the anterior half of the embryo (1) within an inverted U-shaped area surrounding the anterior part of the neural plate and (2) in a region traversing the area of the neural plate, interrupted by the unstained notochordal plate only (Fig. 4C). Cross sections of the inverted U-shaped domain (bracket in Fig. 4I) reveal a strong *BLIMP1* expression in ectodermal cells located medial to the lateral third of the neural plate, leaving the (surface) ectodermal cells near the border of the embryo unstained. Mesodermal and endodermal cells underlying this transverse *BLIMP1* domain express *BLIMP1* to a lesser degree compared to the ectoderm. In addition to the afore mentioned pattern, a strong *BLIMP1* expression is found in the mesoderm underlying the more centrally localized unstained neural ectoderm, while the neural groove and notochord are not labeled (Fig. 4I). The ventral layer (endoderm) located beneath the *BLIMP1*-positive mesoderm cells shows a weak *BLIMP1* expression as well (Fig. 4I).

Less apparent than the prominent anterior domain but closely related to the posterior domain connected with PGC differentiation, *BLIMP1*-expressing cells are also seen in the branched posterior domains which are connected across the posterior pole of the embryo (Fig. 4C, E). Sections of this area display single *BLIMP1*-expressing cells in the mesodermal compartment located inside the border of the embryo which can still be morphologically defined by the difference in cellular height between (surface) ectoderm and trophoblast. Lying in close vicinity to the ventral layer (Fig. 4J, L) and to the yolk sac epithelium, the position of these *BLIMP1*-expressing cells resembles the one of primordial germ cells which can be identified by the monoclonal antibody PG2 directed against a germ cell-specific mitochondria-associated antigen (Fig. 4D). Higher magnification shows the cytoplasmic localization of the immunostaining in single dispersed cells localized within these posterior domains (Fig. 4K). A recalculated orthogonal view (Fig. 4M) of the original fluorescent image stack shows single cells with cytoplasmic fluorescence surrounding DAPI-stained nuclei. These cells are localized in the mesodermal compartment close to the ventral layer (endoderm), which is barely visible in this *z*-sectional view due to the flat configuration of its nuclei, but which can be easily identified in the corresponding series of *xy*-sections (not shown).

Discussion

Next to the mouse, the rabbit is now the second mammal in which pivotal members of the regulatory network involved in the specification of the germline are known to be expressed in a plausible time window and spatial distribution during early gastrulation and neurulation stages: Coincident with the definition of the anterior–posterior body axis at the pregastrulation stage 1, the signaling molecule *BMP2* precedes the transcriptional repressor *BLIMP1* to be switched on in individual posterior epiblast cells at stage 2. Only then, and coincident with the formation of the primitive streak at stage 3, comes the partner signaling molecule *BMP4*—known to be absolutely necessary for germline differentiation in the mouse—into play (see Fig. 5). Chronology and topography of rabbit germline specification thus show subtle but significant differences to that seen in the mouse.

BMP mRNA and PGC detection

Although *BMP2* and *BMP4* are closely related members of the same TGF-ß subfamily (Kingsley 1994; approximately 62% matching bases in the protein coding part of the rabbit cDNAs—GenBank entry NM_001082650.1 and XM_002718254.1), false cross hybridization of our probes seems improbable because (1) portions of sequence identity are relatively short—the maximal non-interrupted stretch had 23 neighboring base pairs—and they are always separated by non-matching sequence parts and (2) the observed in situ hybridization patterns of *BMP2* and *BMP4* differ markedly with regard to their distribution in the embryonic disc and the cell layers. Furthermore, *BLIMP1*-positive mesoderm cells, although not proven by double labeling and colocalization, are considered to be precursors of primordial germ cells as they show—from gastrulation stage 4 onwards—a distribution identical to the one seen with the PG2 antibody known to be specific for PGCs throughout embryonic development in the rabbit (Weckelmann et al. 2008).

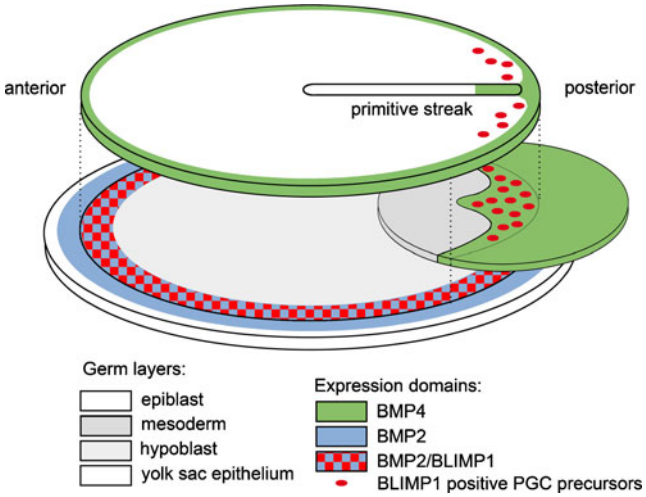

Fig. 5 Schematic summary of expression domains relevant for mammalian germ cell specification ("blimping"). The expression patterns of *BMP2* (*blue*), *BMP4* (*green*) and *BLIMP1* (*red*) are depicted in the germ layers of an advanced stage 3 rabbit embryo. Most intensive *BMP4* expression is found in the mesoderm, which can be separated morphologically into an extraembryonic and an embryonic part by the border between epiblast and trophoblast (trophoblast was omitted from the scheme; cf. Fig. 2B, C). The *BMP4*-positive embryonic mesoderm coincides with the presence of *BLIMP1*-positive germ cell precursors which may therefore define a PGC niche in the rabbit embryo. Less intensive *BMP4* expression is present in the marginal epiblast and the posterior primitive streak, and no expression is found in the hypoblast at this developmental stage. *BMP2* expression, which starts at stage 1, colocalizes with *BLIMP1* (*checkered blue and red*) at stage 3 in the marginal hypoblast and extends into the neighboring yolk sac epithelium (cf. Figs. 1C, D and 3D)

Comparative *BMP2* dynamics

Prior to gastrulation, the most striking *BMP2* expression pattern is the narrow ring-shaped region of "marginal hypoblast" at the periphery of the embryonic disc, which is characterized by attachment, and interaction, of different embryonic tissues and cells (epiblast and trophoblast versus hypoblast and yolk sac epithelia) to create the environment for local differentiation. This pattern is in agreement with findings observed in the mouse embryo (Coucouvanis and Martin 1999) where one can see a stronger reaction near the border between epiblast and extraembryonic ectoderm. Similarly, the broadening of the *BMP2* expression in the posterior hypoblast of the stage 3 rabbit embryo after the onset of gastrulation is in agreement with a stronger *BMP2* expression at the (posterior) side where the primitive streak is forming in the mouse (Ying and Zhao 2001). Higher spatial and temporal resolution made possible by the flat mammotypical embryonic disc of the rabbit reveals, however, that the anterior–posterior differentiation in the *BMP2* expression pattern starts two stages earlier (at stage 1) than seen in the mouse, and is therefore subject to signaling instructions originating in the seemingly symmetrical embryonic disc (cf. eccentric *BLIMP1* expression at stage 0)

The central weak *BMP2* expression also fits the pattern in the mouse visceral endoderm and may be considered to be "leaky" expression. The two extraembryonic domains in the rabbit, one in cuboidal cells near the boundary and the other one in cells with a flat morphology further afar from the embryonic disc, correspond to the cuboidal *BMP2*-expressing proximal visceral endoderm of the mouse embryo at E7.5 (Lyons et al. 1995) and possibly to the parietal endoderm (Reichert's membrane), which is attached to maternal tissues in the mouse and therefore mostly lost prior to in situ hybridization.

BMP2-expressing mesoderm originating from anterior parts of the primitive streak during mid-gastrulation stages, i.e., from the perinodal mesoderm at stage 4, generates a crescent-like domain in agreement with a crescent-shaped *BMP2* expression in the mouse in the anterior part of the embryonic disc (Biben et al. 1998). Finally, *BMP2* expression in the extraembryonic mesoderm of gastrulating and neurulating rabbit embryos corresponds to the *BMP2* expression in the amniotic folds and the chorion of the mouse (Zhang and Bradley 1996).

Comparative *BMP4* dynamics

BMP4 expression starting 5 to 8 h after *BMP2* expression in both the outermost cells of the epiblast and the hypoblast most probably overlap with the area of the *BMP2*-expressing marginal hypoblast and can be taken as a sign of the well-known cooperation of these molecules at the site of their cognate receptors (Chuva de Sousa Lopes et al. 2004) and downstream signaling cascades. *BMP4* expression continuing in the marginal epiblast and mesoderm until neurulation stages (stage 5) is in agreement with data obtained from mouse trophectoderm (Coucouvanis and Martin 1999; Ben-Haim et al. 2006) and extraembryonic mesoderm (Winnier et al. 1995; Lawson et al. 1999). The former will be discussed below in connection with the definition of embryonic borders; the latter on the other hand shows striking, unexplained change of expression at the lateral embryonic disc border where mesoderm cells do not change their morphology as they cross that border on the way from the primitive streak to extraembryonic sites (e.g., to help the formation of the amniotic folds).

Known inhibitors of *BMP4* function are cerberus and cerberus-like molecules (Piccolo et al. 1999); therefore, it is reasonable to assume that the expression of rabbit Cerl (Idkowiak et al. 2004) in the anterior part of the primitive streak restricts the *BMP4* expression to the posterior primitive streak.

Comparative *BLIMP1* dynamics

While the onset of the *BLIMP1* expression in the rabbit hypoblast at stage 1 corresponds to the one observed in the murine visceral endoderm (E5.5; Ohinata et al. 2005), the anterior-posterior asymmetry and the preceding weak and complex expression pattern in all cell layers prior to axial differentiation at stage 0 is novel and points to a molecular differentiation network implementing the early body plan. However, the ring-like *BLIMP1* expression in the stage 2 hypoblast matches the one in the visceral endoderm at the embryonic–extraembryonic junction of the mouse embryo (Vincent et al. 2005) and corresponds to *BMP2*-expressing marginal hypoblast cells with the intriguing possibility of a colocalization and a cause–effect relationship of the two molecules within the same cell (cf. Fig. 5).

BLIMP1-expressing epiblast cells near the posterior boundary of stage 2 and 3 embryonic discs, again, fit the mouse data (Ohinata et al. 2005) and suggest that there are upstream signaling molecules that either advance or inhibit the susceptibility of the posterior or anterior epiblast, respectively, to express *BLIMP1*. These factors would also be responsible for enabling the "blimping" process symmetrically on both sides of the midline. Possible candidates for implementing this axial differentiation might be found in the signaling molecules involved in early anterior/posterior axis formation like *Cer1*, *Dkk1*, or *Wnt3* (Idkowiak et al. 2004), which are known to provide epiblast cells with the ability to respond to *BMP* signals in the mouse (Ohinata et al. 2009). This congruence to the mouse expression pattern (Ohinata et al. 2005) suggests that these *BLIMP1*-expressing epiblast cells are the earliest precursors of the rabbit primordial germ cells which is further supported by the appearance of *BLIMP1*-positive cells in the mesoderm of later developmental stages (stages 4–6) at numbers and positions matching those of PGCs identified by a germline specific antibody (Schäfer-Haas and Viebahn 2000; Weckelmann et al. 2008). To determine numbers of PGC precursors versus specified PGCs further, markers such as *stella* (Saitou et al. 2002) and *Prdm14* (Yamaji et al. 2008) need to be analyzed in the rabbit; however, preliminary experiments in the rabbit (BP unpublished) show that *PRDM14* is expressed in the anterior epiblast in early developmental stages (which is similar to the situation in the mouse: Yamaji et al. 2008) but apparently not in PGCs.

Apart from its role in PGC development, *BLIMP1* expression in early blood islands of the rabbit, although not detected in comparable mouse embryos (Ohinata et al. 2005), corresponds to endothelial expression at later developmental stages (E9.5) found to be essential for the survival of the embryo (Vincent et al. 2005). The intensive but enigmatic *BLIMP1* expression in the mesoderm at the midbrain/hindbrain junction and in the epidermal ectoderm is possibly also found in the mouse (cf. Fig. 3a, b in Vincent et al. 2005).

The evidence for a mammalian germ cell niche

Timing and spatial distribution of gene expression in the rabbit support the evidence of a functional significance of the *BMP–BLIMP1* connection for PGC lineage segregation in general, but single *BLIMP1*-positive cells surrounded by complete ring of *BLIMP1*-negative ones at stages 2 and 3 (cf. Fig. 5) suggest that the initial step for the successful segregation of PGCs may be a lateral inhibition event in single cells similar to neuroblast generation in Drosophila as the result of the Notch–Delta signaling pathway (Axelrod 2010). Complexity is added to the process as it occurs almost simultaneously with the singling out of presumptive mesoderm cells within the epiblast layer in the same location, the posterior gastrula extension (PGE) area: 10 to 15 single epiblast cells of the PGE express the mesodermal master control gene *brachyury* at stage 2 (Viebahn et al. 2002), i.e., at a time when the first few *BLIMP1*-positive epiblast cells appear at the posterior periphery of the PGE area; at stage 3, a handful of *BLIMP1*-positive cells occupy the very same region as the strong *brachyury* expression domain overlying the posterior half of the emerging primitive streak (cf. Fig. 4c, d in Viebahn et al. 2002 with Fig. 5 in this paper). However, singling out of PGCs through the Notch–Delta pathway is in line with observation that PGCs are single cells in later phases of their development, too, as for example during migration to the genital ridge. The fact that early definitive germ cells are stably surrounded by somatic cells also fits the principle of somatic supporting cells closely engaged in the generation, migration, and differentiation of germ cells, a phenomenon frequently observed throughout the animal kingdom (cf. Wawersik et al. 2005; Richardson and Lehmann 2010; Dudley et al. 2010). The concept of lateral inhibition comes as a surprise, though, in view of the concept of the high *fragilis* "concentration" thought to be necessary in the center of the initial clutch of presumptive PGCs at the base of the allantois in the mouse (Saitou et al. 2002). One explanation for this discrepancy between mouse and rabbit may be that the latter mechanism may probably be specific to rodents with their specific topography and timing of an allantois required for early implantation and bridging the gap created early between the embryo and the chorion by the rodent-specific cavity in the ectoplacental cone (Kaufman 1992). The human embryo at gastrulation, on the other hand, has a mammotypical flat embryonic disc and a delayed and rudimentary allantoic development (O'Rahilly and Müller 1987), making a *fragilis*-dependent allantoic germ cell niche an unlikely proposition for human development, too. The

possibility that the allantoic cluster of PGCs represents, in fact, a "cul de sac" for germ cells and that successful development proceeds only for those having entered posterior hindgut or yolk sac endoderm prior to emigration into the base of the allantois has been raised before on the basis of live imaging of PGCs in the mouse (Anderson et al. 2000). Clustering is, of course, a normal and typical mechanism for synchronization of germ cells in a broad variety of animal species, including the human, once germ cells have arrived in the genital ridge and during gametogenesis (cf. Greenbaum et al. 2009).

Acknowledgments We express our gratitude to Kirsten Falk-Stietenroth, Heike Faust, and Irmgard Weiß for their excellent and dedicated technical assistance.

References

Abramoff MD, Magelhaes PJ, Ram SJ (2004) Image processing with ImageJ. Biophotonics International 11:36–42

Ancelin K, Lange UC, Hajkova P, Schneider R, Bannister AJ, Kouzarides T, Surani MA (2006) Blimp1 associates with Prmt5 and directs histone arginine methylation in mouse germ cells. Nat Cell Biol 8:623–630

Anderson R, Copeland TK, Scholer H, Heasman J, Wylie C (2000) The onset of germ cell migration in the mouse embryo. Mech Dev 91:61–68

Axelrod JD (2010) Delivering the lateral inhibition punchline: it's all about the timing. Sci Signal 3:38

Ben-Haim N, Lu C, Guzman-Ayala M, Pescatore L, Mesnard D, Bischofberger M, Naef F, Robertson EJ, Constam DB (2006) The nodal precursor acting via activin receptors induces mesoderm by maintaining a source of its convertases and BMP4. Dev Cell 11:313–323

Biben C, Stanley E, Fabri L, Kotecha S, Rhinn M, Drinkwater C, Lah M, Wang CC, Nash A, Hilton D, Ang SL, Mohun T, Harvey RP (1998) Murine cerberus homologue mCer-1: a candidate anterior patterning molecule. Dev Biol 194:135–151

Blum M, Andre P, Muders K, Schweickert A, Fischer A, Bitzer E, Bogusch S, Beyer T, van Straaten HW, Viebahn C (2007) Ciliation and gene expression distinguish between node and posterior notochord in the mammalian embryo. Differentiation 75:133–146

Chang H, Matzuk MM (2001) Smad5 is required for mouse primordial germ cell development. Mech Dev 104:61–67

Chiquoine AD (1954) The identification, origin, and migration of the primordial germ cells in the mouse embryo. Anat Rec 118:135–146

Chuva de Sousa Lopes SM, Roelen BA (2008) Primordial germ cell specification: the importance of being 'blimped'. Histol Histopathol 23:1553–1561

Chuva de Sousa Lopes SM, Roelen BA, Monteiro RM, Emmens R, Lin HY, Li E, Lawson KA, Mummery CL (2004) BMP signaling mediated by ALK2 in the visceral endoderm is necessary for the generation of primordial germ cells in the mouse embryo. Genes Dev 18:1838–1849

Chuva de Sousa Lopes SM, Hayashi K, Surani MA (2007) Proximal visceral endoderm and extraembryonic ectoderm regulate the formation of primordial germ cell precursors. BMC Dev Biol 7:140

Coucouvanis E, Martin GR (1999) BMP signaling plays a role in visceral endoderm differentiation and cavitation in the early mouse embryo. Development 126:535–546

Dudley B, Palumbo C, Nalepka J, Molyneaux K (2010) BMP signaling controls formation of a primordial germ cell niche within the early genital ridges. Dev Biol 343:84–93

Extavour CG, Akam M (2003) Mechanisms of germ cell specification across the metazoans: epigenesis and preformation. Development 130:5869–5884

Greenbaum MP, Iwamori N, Agno JE, Matzuk MM (2009) Mouse TEX14 is required for embryonic germ cell intercellular bridges but not female fertility. Biol Reprod 80:449–457

Idkowiak J, Weisheit G, Plitzner J, Viebahn C (2004) Hypoblast controls mesoderm generation and axial patterning in the gastrulating rabbit embryo. Dev Genes Evol 214:591–605

Kaufman MH (1992) The atlas of mouse development. Academic, London

Kingsley DM (1994) The TGF-beta superfamily: new members, new receptors, and new genetic tests of function in different organisms. Genes Dev 8:133–146

Kurimoto K, Yabuta Y, Ohinata Y, Shigeta M, Yamanaka K, Saitou M (2008) Complex genome-wide transcription dynamics orchestrated by Blimp1 for the specification of the germ cell lineage in mice. Genes Dev 22:1617–1635

Lawson KA, Hage WJ (1994) Clonal analysis of the origin of primordial germ cells in the mouse. Ciba Found Symp 182:68–84, discussion 84–91

Lawson KA, Dunn NR, Roelen BA, Zeinstra LM, Davis AM, Wright CV, Korving JP, Hogan BL (1999) Bmp4 is required for the generation of primordial germ cells in the mouse embryo. Genes Dev 13:424–436

Lyons KM, Hogan BL, Robertson EJ (1995) Colocalization of BMP 7 and BMP 2 RNAs suggests that these factors cooperatively mediate tissue interactions during murine development. Mech Dev 50:71–83

McLaren A (2003) Primordial germ cells in the mouse. Dev Biol 262:1–15

Mossman HW (1937) Comparative morphogenesis of the fetal membranes and accessory uterine structures. Contrib Embryol Carnegie Inst 26:129–246

Nieuwkoop PD, Sutasurya LA (1979) Primordial germ cells in the chordates: embryogenesis and phylogenesis. Cambridge University Press, Cambridge

Ohinata Y, Payer B, O'Carroll D, Ancelin K, Ono Y, Sano M, Barton SC, Obukhanych T, Nussenzweig M, Tarakhovsky A, Saitou M, Surani MA (2005) Blimp1 is a critical determinant of the germ cell lineage in mice. Nature 436:207–213

Ohinata Y, Ohta H, Shigeta M, Yamanaka K, Wakayama T, Saitou M (2009) A signaling principle for the specification of the germ cell lineage in mice. Cell 137:571–584

O'Rahilly R, Müller F (1987) Developmental stages in human embryos. Publication 637. Carnegie Institution of Washington, Washington DC

Piccolo S, Agius E, Leyns L, Bhattacharyya S, Grunz H, Bouwmeester T, De Robertis EM (1999) The head inducer Cerberus is a multifunctional antagonist of Nodal, BMP and Wnt signals. Nature 397:707–710

Püschel B, Viebahn C (2010) Whole-mount in situ immunofluorescence of early rabbit embryos. Cold Spring Harb Protoc. doi:10.1101/pdb.prot5354

Richardson BE, Lehmann R (2010) Mechanisms guiding primordial germ cell migration: strategies from different organisms. Nat Rev Mol Cell Biol 11:37–49

Saitou M, Yamaji M (2010) Germ cell specification in mice: signalling, transcription regulation, and epigenetic consequences. Reproduction 139:931–942

Saitou M, Barton SC, Surani MA (2002) A molecular programme for the specification of germ cell fate in mice. Nature 418:293–300

Schäfer-Haas A, Viebahn C (2000) The germ cell epitope PG-2 is expressed in primordial germ cells and in hypoblast cells of the gastrulating rabbit embryo. Anat Embryol (Berl) 202:13–23

Snow MH (1981) Autonomous development of parts isolated from primitive-streak-stage mouse embryos. Is development clonal? J Embryol Exp Morphol 65:269–287

Tam PP, Zhou SX (1996) The allocation of epiblast cells to ectodermal and germ-line lineages is influenced by the position of the cells in the gastrulating mouse embryo. Dev Biol 178:124–132

Tanaka SS, Matsui Y (2002) Developmentally regulated expression of mil-1 and mil-2, mouse interferon-induced transmembrane protein like genes, during formation and differentiation of primordial germ cells. Mech Dev 119(Suppl 1):S261–S267

Turner CA Jr, Mack DH, Davis MM (1994) Blimp-1, a novel zinc finger-containing protein that can drive the maturation of B lymphocytes into immunoglobulin-secreting cells. Cell 77:297–306

Viebahn C, Miething A, Wartenberg H (1998) Primordial germ cells of the rabbit are specifically recognized by a monoclonal antibody labelling the perimitochondrial cytoplasm. Histochem Cell Biol 109:49–58

Viebahn C, Stortz C, Mitchell SA, Blum M (2002) Low proliferative and high migratory activity in the area of Brachyury expressing mesoderm progenitor cells in the gastrulating rabbit embryo. Development 129:2355–2365

Vincent SD, Dunn NR, Sciammas R, Shapiro-Shalef M, Davis MM, Calame K, Bikoff EK, Robertson EJ (2005) The zinc finger transcriptional repressor Blimp1/Prdm1 is dispensable for early axis formation but is required for specification of primordial germ cells in the mouse. Development 132:1315–1325

Wawersik M, Milutinovich A, Casper AL, Matunis E, Williams B, Van Doren M (2005) Somatic control of germline sexual development is mediated by the JAK/STAT pathway. Nature 436:563–567

Weckelmann A, Viebahn C, Püschel B (2008) Subcellular redistribution of the mitochondrial PG2 epitope during development from cleavage to primordial germ cell formation in the rabbit embryo. Sex Dev 2:31–42

Weisheit G, Mertz D, Schilling K, Viebahn C (2002) An efficient in situ hybridization protocol for multiple tissue sections and probes on miniaturized slides. Dev Genes Evol 212:403–406

Winnier G, Blessing M, Labosky PA, Hogan BL (1995) Bone morphogenetic protein-4 is required for mesoderm formation and patterning in the mouse. Genes Dev 9:2105–2116

Witschi E (1948) Migration of the germ cells of human embryos from the yolk sac to the primitive gonadal fold. Contrib Embryol Carnegie Inst 32:67–80

Yabuta Y, Kurimoto K, Ohinata Y, Seki Y, Saitou M (2006) Gene expression dynamics during germline specification in mice identified by quantitative single-cell gene expression profiling. Biol Reprod 75:705–716

Yamaguchi S, Kimura H, Tada M, Nakatsuji N, Tada T (2005) Nanog expression in mouse germ cell development. Gene Expr Patterns 5:639–646

Yamaji M, Seki Y, Kurimoto K, Yabuta Y, Yuasa M, Shigeta M, Yamanaka K, Ohinata Y, Saitou M (2008) Critical function of Prdm14 for the establishment of the germ cell lineage in mice. Nat Genet 40:1016–1022

Ying Y, Zhao GQ (2001) Cooperation of endoderm-derived BMP2 and extraembryonic ectoderm-derived BMP4 in primordial germ cell generation in the mouse. Dev Biol 232:484–492

Ying Y, Liu XM, Marble A, Lawson KA, Zhao GQ (2000) Requirement of Bmp8b for the generation of primordial germ cells in the mouse. Mol Endocrinol 14:1053–1063

Ying Y, Qi X, Zhao GQ (2001) Induction of primordial germ cells from murine epiblasts by synergistic action of BMP4 and BMP8B signaling pathways. Proc Natl Acad Sci U S A 98:7858–7862

Yoshimizu T, Obinata M, Matsui Y (2001) Stage-specific tissue and cell interactions play key roles in mouse germ cell specification. Development 128:481–490

Zhang H, Bradley A (1996) Mice deficient for BMP2 are nonviable and have defects in amnion/chorion and cardiac development. Development 122:2977–2986